Microbes and Infection 21 (2019) 456–463

Contents lists available at ScienceDirect

Microbes and Infection

journal homepage: www.elsevier.com/locate/micinf

Original article

The influence of pH on *Staphylococcus saprophyticus* iron metabolism and the production of siderophores

Bianca Silva Vieira de Souza [a], Karla Christina Sousa Silva [a], Ana Flávia Alves Parente [b], Clayton Luiz Borges [a], Juliano Domiraci Paccez [a], Maristela Pereira [a], Célia Maria de Almeida Soares [a], Marcia Giambiagi-deMarval [c], Mirelle Garcia Silva-Bailão [a], Juliana Alves Parente-Rocha [a, *]

[a] Laboratório de Biologia Molecular, Instituto de Ciências Biológicas, Universidade Federal de Goiás, Av. Esperança, ICB2, 74690-900, Goiânia - Goiás, Brazil
[b] Instituto de Biologia, Campus Universitário Darcy Ribeiro, Universidade de Brasília, 70297-400, Brasília – Distrito Federal, Brazil
[c] Laboratório de Microbiologia Molecular, Instituto de Microbiologia Prof. Paulo de Góes, Universidade Federal do Rio de Janeiro, Cidade Universitária, 21941-970, Rio de Janeiro – Rio de Janeiro, Brazil

ARTICLE INFO

Article history:
Received 10 October 2018
Accepted 30 April 2019
Available online 7 May 2019

Keywords:
pH
Iron metabolism
S. saprophyticus
Carboxylate siderophores
Citrate synthase

ABSTRACT

Staphylococcus saprophyticus is a gram-positive coagulase negative bacteria which shows clinical importance due to its capability of causing urinary tract infections (UTI), as well as its ability to persist in this environment. Little is known about how *S. saprophyticus* adapts to the pH shift that occurs during infection. Thus, in this study we aim to use a proteomic approach to analyze the metabolic adaptations which occur as a response by *S. saprophyticus* when exposed to acid (5.5) and alkaline (9.0) pH environments. Proteins related to iron storage are overexpressed in acid pH, whilst iron acquisition proteins are overexpressed in alkaline pH. It likely occurs because iron is soluble at acid pH and insoluble at alkaline pH. To evaluate if *S. saprophyticus* synthesizes siderophores, CAS assays were performed, and the results confirmed their production. The chemical characterization of siderophores demonstrates that *S. saprophyticus* produces carboxylates derived from citrate. Of special note is the fact that citrate synthase (CS) is down-regulated during incubation at acid pH, corroborating this result. This data was also confirmed by enzymatic assay. Our results demonstrate that iron metabolism regulation is influenced by different pH levels, and show, for the first time, the production of siderophores by *S. saprophyticus*. Enzymatic assays suggest that citrate from the tricarboxylic acid cycle (TCA) is used as substrate for siderophore production.

The human microbiota is composed of several species of bacteria which have established a symbiotic relationship with the human host. Despite the symbiotic relationship, these organisms may become pathogenic to the host [1] in specific situations. Among them, *Staphylococcus saprophyticus* is an important species of gram-positive and coagulase negative bacteria [1,2] that can cause urinary tract infections (UTI). *S. saprophyticus* is the second most prevalent cause of UTI, corresponding to 40% of the cases [3], especially in women, and is present in the periurethral region, skin and mucosal ecosystem of the genito-urinary tract [1].

The ability to obtain and stock iron is considered a virulence factor in pathogenic microorganisms since the hosts possess nutritional immunity, in other words, strategies to reduce the availability of iron [4]. The complexation of iron with host proteins, such as hemoglobin, ferritin and transferrin, is a way of depriving pathogens of iron [5]. In *Staphylococcus aureus*, about 30% of proteins depend on metals to perform the role of cofactor [6]. During infection, the host promotes metal starvation – such as Mn and Zn – causing reduced bacterial growth and an increase in neutrophil killing efficiency [7,8].

Human urine has a slightly acid pH that ranges from 5 to 6. When infection by *S. saprophyticus* starts in the urinary tract,

* Corresponding author. Laboratório de Biologia Molecular, Departamento de Bioquímica e Biologia Molecular, Instituto de Ciências Biológicas, Universidade Federal de Goiás, Goiânia - Goiás, 74690-900, Brazil.Fax: +55 62 3521 1110.
E-mail addresses: bianca_svs@hotmail.com (B.S.V. Souza), karlabio@live.com (K.C.S. Silva), afparente@yahoo.com.br (A.F.A. Parente), clbluiz2@gmail.com (C.L. Borges), julianopaccez@gmail.com (J.D. Paccez), maristelaufg@gmail.com (M. Pereira), cmasoares@gmail.com (C.M.A. Soares), marciagm@micro.ufrj.br (M. Giambiagi-deMarval), mirellegarcias@gmail.com (M.G. Silva-Bailão), juparente@gmail.com (J.A. Parente-Rocha).

https://doi.org/10.1016/j.micinf.2019.04.008
1286-4579/

bacterial cells use urea available in the urine to acquire nitrogen. Urea is degraded to carbon dioxide and ammonia by the action of bacterial urease, which leads to an increase in the pH of urine [9]. The pH influences the iron concentration since the acidic pH increases the availability of soluble iron (Fe^{2+}), and at alkaline pHs the insoluble iron (Fe^{3+}) occurs in higher concentrations [10].

There are two basic systems of iron uptake in bacteria: the ferritin iron reduction system and uptake by secretion or acquisition of siderophores. Ferritins are proteins conserved from bacteria to higher eukaryotes. They play a key role in the control of intracellular iron concentrations due to their function of reserving iron in a non-toxic and bioavailable form [11].

Siderophores are low molecular weight iron chelating molecules which are able to remove iron from the carrier proteins (hemoglobin, transferrin and lactoferrin) and transport them into the cytoplasm [12,13]. Microorganisms can produce more than one type of siderophore. The acquisition of siderophores produced by other microbial species has already been described for bacteria such as *Escherichia coli, Salmonella typhimurium,* and *Actinobacillus pleuropneumoniae* [14]. Periplasmic proteins carry the siderophore-iron complexes to ABC (ATP-binding cassette) transporters in the cytoplasmic membrane, which carry them to the cytosol [15].

The production of siderophores in the *Staphylococcus* genus was first reported in *S. hyicus*. The ability of staphyloferrin B to transport iron has also been reported. Staphyloferrin B has been described as a polycarboxylate molecule, synthesized from citrate [16]. *S. aureus* produces two carboxylate siderophore molecules that can capture iron: staphyloferrin A, and staphyloferrin B. It has been suggested that staphyloferrin A is produced from citrate derived from TCA [17], and staphyloferrin B is produced from citrate generated by SbnG, a second CS that is structurally distinct from TCA cycle CS [18]. The acquisition of xenosiderophores in *S. aureus* has also been reported as being dependent on the extracellular surface lipoproteins FhuD1 and FhuD2, as well as the ABC transporter complex FhuCBG which internalizes hydroxamate xenosiderophores [19].

The iron metabolism in coagulase negative *Staphylococcus* spp. is poorly understood. *Staphylococcus epidermidis* produces siderophores, and the genes *sirR* and *sitABC* operon – related to iron acquisition – are regulated in response to iron deprivation [20]. Recently, it was observed that the formation of biofilm in *S. epiderimidis* depends on iron availability [21]. The use of exogenous siderophores – such as exochelin-MS and deferoxamine-B – has been tested in synergistic tests, with antibiotics showing promise in the treatment of resistant gram-positive and gram-negative bacteria [22].

In *S. saprophyticus* there is still no description of how regulation of intracellular iron concentration occurs. Previous *S. saprophyticus* genome analysis noted that this bacteria does not possess siderophore-producing systems [23]. In this study we characterized that pH regulates the expression of proteins related to iron metabolism. We performed *in silico* analysis, and an operon for siderophore production was detected and described. We are showing, for the first time, the production of siderophores in *S. saprophyticus*, demonstrating the production of carboxylates, derived from citrate, produced in the absence of extracellular iron.

1. Material and methods

1.1. Cultivation and cell growth curve of S. saprophyticus

The strain *S. saprophyticus* ATCC 15305 was used in all experiments throughout this study. This strain was cultured in solid Brain Heart Infusion medium (BHI) (Sigma Aldrich, St Louis, MO, USA). One colony was used to perform a pre-inoculum for 16–18 h of incubation at 36 °C under agitation. Then, 1% of this inoculum was used for inoculation of a new inoculum in BHI broth medium until the optical density of 0.7 at 630 nm (OD_{630} 0.7) in spectrophotometry SpectraMax Paradigm (Molecular Devices, Lagerhausstrasse, Austria) was reached. The cells were collected by centrifugation and incubated in BHI broth medium in different conditions: acidic (pH 5.5), neutral (pH 7.0) and alkaline (pH 9.0). The cell growth curve was performed with *S saprophyticus* cells cultured in BHI broth medium by monitoring the OD_{630} for 8 h.

1.2. Protein extraction and sample preparation for mass spectrometry

The proteomic analysis was carried out after 3 h of bacterial culture in acid (5.5), neutral (7) and alkaline (9) pH respectively. Protein extracts were obtained by using glass beads 0.2–0.8 nm (Sigma Aldrich, St Louis, MO, USA). Cells were lysed using Bead Beater (Biospec, Bartlesville, OK, USA) during four cycles of 30 s. After cell lysis, the protein extract was obtained by centrifugation at 10,000*g* for 15 min. The samples were quantified using Bradford reagent (Sigma Aldrich, St Louis, MO, USA) using spectrophotometry SpectraMax Paradigm (Molecular Devices, Lagerhausstrasse, Austria) and then concentrated in a 3 kDa disposable Amicon ultrafilter (Millipore®, Bedford, MA, USA) to obtain the minimum concentration of 1 μg/μL of each protein extract. The integrity of the protein extract obtained was evaluated on SDS-PAGE containing 30 μg of extract from each gel condition evaluated.

A total of 150 μg of each protein extract was used for identification by mass spectrometry. The samples were reduced with 10 mM DTT (GE Healthcare, Piscataway, NJ, USA) for 30 min and also treated with 10 mM iodoacetamide (GE Healthcare, Piscataway, NJ, USA) for alkylation. After this treatment, the proteins were incubated with 20 ng trypsin (Promega, Madison, WI, USA) for 16 h at 36 °C for digestion. The samples were then treated with trifluoroacetic acid (TFA) 0.1% (Sigma Aldrich, St Louis, MO, USA) and purified in resin C18 ZipTips (Millipore, Darmstadt, Germany). The resins were equilibrated prior to use with acetonitrile (ACN) (Sigma Aldrich, St Louis, MO, USA), followed by washing with the following solutions: (1) 80% ACN and TFA 0.1% (2) 50% ACN and 0.1% TFA, (3) 30% ACN and 0.1% TFA, and finally (4) 0.1% TFA. Peptides were linked to ZipTips for 10 consecutive pipettings of 10 μL samples. After binding of the peptide on the resin, impurities were removed by washing with 0.1% TFA, and the peptide was eluted with 50% ACN and 0.1% TFA, followed by elution with 80% ACN with TFA 0.1%. The two eluates were combined for concentration using the vacuum centrifuge Concentrator plus (Eppendorf, Hamburg, Germany).

1.3. Mass spectrometry for the identification of S. saprophyticus proteins

The samples were analyzed after separation by nano liquid chromatography (LC) Nano Acquity UPLC (Waters Corporation, USA) by nano-electrospray mass spectrometer source (ESI) MS/MS by applying 1.5 kV and flow volume of 1 μL/min in unit SYNAPT Q-TOF (Waters Corporation, USA). Homology analysis was performed on databases using ProteinLynx 2.3 software (Waters Corporation, USA). Uniprot (http://www.uniprot.org) was used for functional classification. Protein expression analyses were performed by applying the PLGS ExpressionE algorithm to a statistically-significant list corresponding to up- and down-regulation ratios among the different groups. The same algorithm was applied to the proteins detected in only one experimental condition.

1.4. CS enzymatic assay

The enzymatic activity of the CS was determined as previously described [24]. The reaction of 5,5-dithiobis-2-nitrobenzoate (DTNB) with CoA, forming 5-thio-2-nitrobenzoic acid, gives a yellowish coloration to the reaction mixture detected at 412 nm. Final concentrations of 50 mM Tris-HCl, pH 8.0, 0.2 mM acetyl-CoA (Sigma Aldrich, St Louis, MO, USA), 1 mM oxaloacetate (Sigma Aldrich, St Louis, MO, USA), and 1 mM DTNB (Sigma Aldrich, St Louis, MO, USA) were added in a reaction of 150 μl. A total of 10 μg of protein extract was used and the reading was completed after 40 min. The amount of CoA formed per minute was obtained using a DTT standard curve, varying the concentration from 0.5 μM to 25 μM. The experiment was performed in technical triplicate and standard error of the mean obtained.

1.5. Evaluation of S. saprophyticus cell growth under iron deprivation

Every glassware used in the growth assay was treated with Nitric Acid 10%. The medium used was treated with Quelex (Sigma Aldrich, St Louis, MO, USA) for 1 h and filtered prior to use. For the growth curve of *S. saprophyticus* in staphylococcal siderophore detection medium (SSD medium) in the presence and absence of iron, a colony was pre-inoculated in SSD medium [25] with 2 mM of iron and incubated for 16–18 h at 36 °C under agitation. A total of 0.5% of the pre-inoculum was used in a new inoculum in SSD medium with the appropriate iron concentrations established for the curve: 0, 0.1, 0.5, 1, 5 and 10 μM. The cells were incubated at 36 °C under agitation, OD_{630} and monitored for 2 h each over a period of 72 h in spectrophotometry SpectraMax Paradigm (Molecular Devices, Lagerhausstrasse, Austria). The experiment was performed in triplicate using a 96 well plate.

1.6. Effect of iron deprivation in S. saprophyticus during interaction with macrophage cells

S. saprophyticus strain ATCC15305 was incubated in SSD medium [25] with and without iron for 18 h at 36 °C under agitation. These cells were washed with RPMI medium (Sigma Aldrich, St Louis, MO, USA) and used for a macrophage phagocytosis assay to evaluate the effect of iron depletion on the survival of *S. saprophyticus* during phagocytosis. Macrophages J774 lineage cultured in RPMI medium and previously activated with gamma interferon for 24 h were used for infection with *S. saprophyticus* cells previously cultured in an iron-deprived environment for 48 h, and those not deprived of iron (control). A MOI of 50:1 (bacteria:macrophage) was used. After 2 h, the macrophages were lysed and the bacteria internalized, recovered and plated on BHI agar medium containing novobiocin 5 μg/ml (Sigma Aldrich, St Louis, MO, USA) for counting colony forming units (CFU).

1.7. In silico analysis to predict operon of siderophore production

The *in silico* analysis to predict the operon used for siderophore prediction was performed by using the Operon prediction online tool (http://operondb.cbcb.umd.edu/cgi-bin/operondb/taxon_list.cgi). Homology analysis was performed using the NCBI blast tool (https://blast.ncbi.nlm.nih.gov/Blast.cgi).

1.8. Evaluation of siderophore production by S. saprophyticus by using CAS assay

The CAS (Chrome Azurol S) was employed for the detection of siderophores, according to the protocol already standardized by our research group [26]. Stock solutions were prepared: HDTMA (hexadecyltrimethylammonium bromide) (Fisher Scientific) 10 mM; 1 mM $FeCl_3$ $6H_2O$ solution (Sigma Aldrich) in 10 mM HCl; and 2 mM CAS (Sigma Aldrich). The CAS assay solution was prepared by adding 6 mL HDTMA, 1.5 ml iron solution and 7.5 ml CAS solution. In another flask were added 4.3 g of piperazine (PIPES) (Sigma Aldrich) in water and 6.25 ml of 12 M HCl. This buffer was added to the first vial containing CAS solution and the volume filled with ultrapure water.

To determine the presence of siderophores, 500 μl of *S. saprophyticus* culture supernatant without Fe (previously centrifuged at 13,400 g for 5 min) and 500 μl of the CAS solution were mixed. The same volume of a reference sample, consisting of sterile culture medium, was also mixed with CAS solution. The change of color was visually detected [27].

1.9. Chemical characterization of siderophores produced by S. saprophyticus cells

The solution for chemical characterization was prepared by adding 3 drops of 2 N NaOH and 1 drop of phenolphthalein. Water was added until a light pink color developed. Afterwards, culture supernatant of *S. saprophyticus* in SSD medium without iron was added to the phenolphthalein solution. Disappearance of pink color indicates the presence of carboxylate siderophores [28].

2. Results

2.1. Evaluation of cell growth during acid, neutral and alkaline pH

In order to evaluate the cell growth of *S. saprophyticus* in acid, neutral and alkaline pH, we analyzed a cell growth curve over a period of 8 h in the pHs 5.5, 7.0 and 9.0 respectively, as described above. The result is shown in Supplementary Fig. 1. No difference in the cell growth was observed in the first 3 h of incubation. However, we observed a discreet reduction in the cell growth rate of *S. saprophyticus* at pH 5.5 after 4 h, maintained for 8 h. In order to ensure the same quantity of cells, we used the time of 3 h to evaluate the proteomic response of *S. saprophyticus* to acid and alkaline pH.

2.2. S. saprophyticus' response to acid and alkaline incubation

We used a proteomic approach to evaluate the response of *S. saprophyticus* to acid and alkaline pH exposure after 3 h. We established a 35% cut off in the protein expression to evaluate which proteins were up- and down-regulated in response to pH treatment. A total of 27 proteins were positively regulated and 90 were negatively regulated in response to acid pH treatment. After incubation in alkaline pH, *S. saprophyticus* up-regulated 28 proteins and down-regulated 64 proteins. These regulated proteins are described in Supplementary Tables 1 and 2. Of special note is the fact that during acid growth conditions, *S. saprophyticus* up-regulated two subunits of the urease system. In contrast, *S. saprophyticus* down-regulated three urease subunits during incubation in alkaline pH. Since urease activity promotes alkalization through ammonia production, the up-regulation during acid incubation probably occurred in order to promote alkalization, and the down-regulation of urease subunits probably occurred to avoid this process.

Seven enzymes of the glycolytic pathway, as well as the L-lactate dehydrogenase, were down-regulated during *S. saprophyticus* incubation in acid pH. This is probably a strategy to avoid increasing acidification caused by lactic production. Acidic conditions, on the other hand, led to up-regulation of fatty acid degradation. This is

shown by the induction of acyl CoA thioesterase that is likely used to maintain the bacterial metabolism in an acid environment (Supplementary Table 1).

Among the adaptations of *S. saprophyticus* to alkaline pH, we noted the up-regulation of the gluconeogenesis pathway and glycine metabolism, and the down-regulation of glycolysis. The gluconeogenesis pathway probably supplies glucose inside the cell that can be used for cell wall and capsule structures. It also supplies energy metabolism. Glycine metabolism is related to an anti-oxidative defense metabolism in bacteria, such as *Pseudomonas fluorescens* [29] and it is especially important since several anti-oxidative proteins are iron-dependent, such as Mn/Fe superoxide dismutase, and because the availability of soluble iron is lower at alkaline pH (Supplementary Table 2). The regulation of these pathways and proteins are shown in a heat map that evidences *S. saprophyticus* down- and up-regulations occurring after alkaline treatment of *S. saprophyticus* cells (Fig. 1).

2.3. S. saprophyticus *regulates iron metabolism during acidic and alkaline growth conditions*

The main metabolic alteration observed in the proteomic analysis was related to iron metabolism (acquisition, storage and utilization) during both acid and alkaline treatments. The proteins related to iron metabolism, or those dependent on iron, which were regulated by pH in *S. saprophyticus*, are shown in Table 1.

At lower pH, soluble Fe^{2+} predominates while the insoluble form (Fe^{3+}) is predominant at alkaline pHs [30]. Thus, microorganisms adapt to iron toxicity at lower pH and deal with iron deprivation under alkaline conditions. The iron-dependent protein catalase is up-regulated, since iron is available in higher concentrations and may trigger oxidative stress. Table 1 shows that at acid pH, *S. saprophyticus* down-regulates a putative heme-dependent peroxidase, which has been described in *S. aureus* as playing a role in iron acquisition, the chelation of heme and the intake of this molecule [31]. In addition, *S. saprophyticus* down-regulates an intracellular ferritin, which is known in several microorganisms, such as *E. coli*, as a storage protein that provides internal iron stock to the cell and confers protection against metal toxicity and oxidative stress [32]. In this sense, the protein deaminase porphobilinogen – involved in heme synthesis [33] – and CS – involved in the generation of citrate used for carboxylate siderophores [17] – as well as the protein SufC – involved in the Fe–S cluster assembly [34] – are down-regulated in *S. saprophyticus* during acid incubation.

A contrasting metabolic response was detected in *S. saprophyticus* during alkaline incubation. The bacterial cells up-regulate an ABC transporter for siderophores, probably to increase iron uptake. On the other hand, *S. saprophyticus* down-regulates the iron-dependent protein superoxide dismutase (SOD), as well as two flavohemoproteins that are involved in iron stocking and oxidative/nitrosative stress response [35].

2.4. S. saprophyticus *presents cell growth during iron deprivation and in higher concentrations of iron*

With the objective to investigate *S. saprophyticus* behavior under iron deprivation conditions and in different metal concentrations, growth analysis in SSD was performed. Medium was supplemented, or not, with 0.1, 0.5, 1, 5 and 10 μM of iron. Bacterial growth was checked for 72 h. As shown in Supplementary Fig. 2, *S. saprophyticus* is able to grow under iron deprivation, as well as in all iron concentrations analyzed, suggesting the bacteria present mechanisms to stock and mobilize the iron.

2.5. *Iron deprivation reduces the survival of* S. saprophyticus *during interaction with macrophage cells*

Since the hosts possess strategies to reduce the availability of iron during infection, pathogens are able to stock iron in organic molecules, such as flavohemoproteins [35], and in inorganic clusters, named Fe–S clusters [36]. The importance of iron during the interaction of *S. saprophyticus* with host cells was evaluated through an interaction assay of *S. saprophyticus* cells with macrophage cells for 2 h. The *S. saprophyticus* cells were pre-incubated in SSD medium without iron for 48 h (to promote utilization of

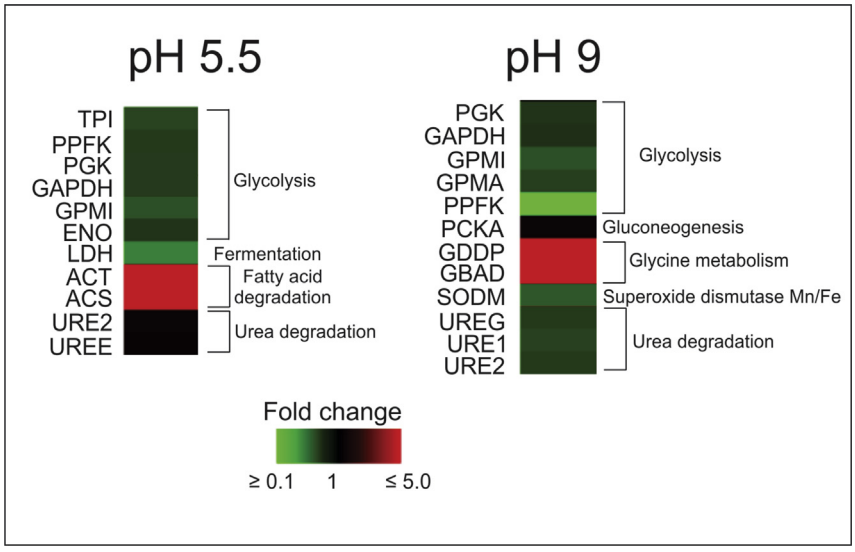

Fig. 1. Heat map of regulated pathways and proteins during acid and alkaline incubation of *S. saprophyticus* cells. Heat map generated by using fold change values. TPI: triosephosphate isomerase; PPFK: 6 phosphofructokinase; PGK: phosphoglycerate kinase; GAPDH: glyceraldehyde 3 phosphate dehydrogenase; GPMI: 2 3 bisphosphoglycerate independent phosphoglycerate mutase; ENO: enolase; LDH: lactate dehydrogenase; ACT: acyl CoA thioesterase; ACS: acyl CoA synthase/ligase; URE2: urease subunit beta; UREE: urease accessory protein subunit E; GPMA: 2 3 bisphosphoglycerate dependent phosphoglycerate phosphomutase; PCKA: phosphoenolpyruvate carboxykinase; GDDP: glycine dehydrogenase decarboxilating P protein; GBAD: glycine betaine aldehyde dehydrogenase; URE1: urease subunit alpha.

Table 1
S. saprophyticus regulated proteins during acid and alkaline treatment related to iron metabolism (acquisition, storage and utilization).

Accession number[a]	Protein description[b]	Relative expression[c]
pH 5.5 - up regulated		
CATA	Catalase	1.42
pH 5.5 - down regulated		
Y2125	Putative heme-dependent peroxidase	0.69
FTN	Ferritin	0.59
LIPA	Lipoyl synthase	0.65
Q49YC5	Citrate synthase	0.25
HEM3	Deaminase porphobilinogen	0.65
pH 9.0 - up regulated		
Q49ZK8	Putative ABC type cobalamin Fe^{3+} siderophore transport system	*
pH 9.0 - down regulated		
LIPA	Lipoil synthase	0.66
HEMH	Ferrochelatase	0.66
SODM	Superoxide dismutase Mn Fe	0.57
Q49UL6	Flavohemoprotein	0.53
Q49WI6	Putative flavohemoprotein	0.57
Q49W53	Putative regulator of iron ABC transporter SufC	0.70

*Unidentified proteins in the control condition.
[a] Protein access number in the UNIPROT database.
[b] Description of the protein according to UNIPROT data.
[c] - Expression of the protein in relation to the control condition (pH7). Modulation of the expression in 35% was considered significant (values ≤ 0.74 and ≥ 1.35).

stocked iron). A control assay was performed with *S. saprophyticus* cells pre-incubated in SSD medium containing iron. The result is shown in Fig. 2. It is possible to note that iron-deprived *S. saprophyticus* cells present a reduced survival rate after interaction with macrophage cells, suggesting that iron stock is important during interaction with the host cells.

2.6. S. saprophyticus *possesses an operon related to siderophore synthesis*

Previous studies have described *S. saprophyticus* as possessing no machinery for siderophore production [23] when compared with operons and the production of staphyloferrin B in *S. aureus*. However, *S. aureus* also possesses an operon related to the staphyloferrin A siderophore, and previous studies have described *S. epidermidis* as possessing an operon that is homologous with the one present in *S. aureus* [21]. We decided, by using *in silico* analysis, to investigate the presence of operons which are homologous with the *S. aureus* operons previously described. Our results show that *S. saprophyticus* possesses one operon that is homologous with an operon from *S. epidermidis* and *S. aureus*; it is related to the production of staphyloferrin A. The *S. saprophyticus* operon is shown in Fig. 3. We could not identify any operons in *S. saprophyticus* that were homologous with operons of *S. aureus* in relation to staphyloferrin B production (data not shown). Our result suggests that, similar to what happens in *S. epidermidis*, *S. saprophyticus* produces only one siderophore, probably derived from citrate.

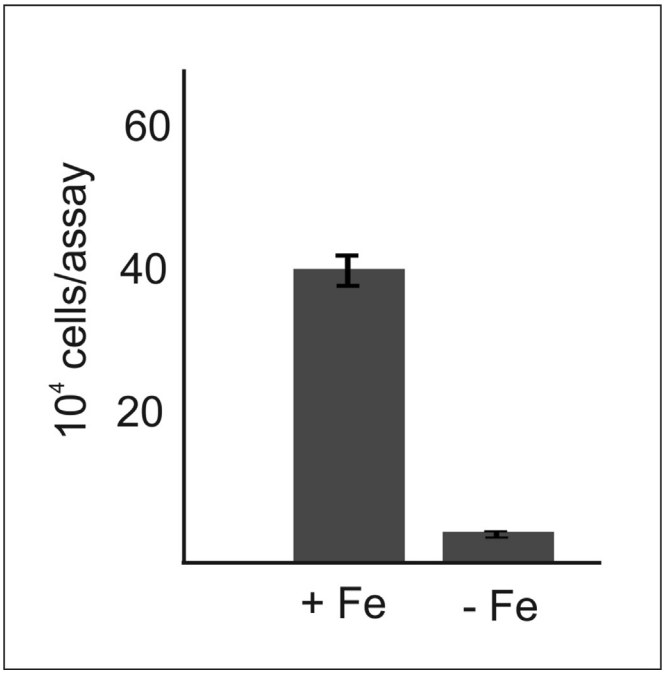

Fig. 2. Survival assay of *S. saprophyticus* cells during interaction with macrophage cells. The *S. saprophyticus* cells were previously cultured in SSD medium without iron (-Fe) and with 10 μM of iron (+Fe) and used to perform the interaction assay with macrophage cells J774. The experiment was performed in triplicate and standard error of the mean obtained.

2.7. S. saprophyticus *CS is down-regulated after incubation in acid pH and strongly up-regulated after iron deprivation*

Since *S. aureus* synthesizes siderophores (staphyloferrin A and B) from citrate (carboxylate siderophores) [16] and since we detected, in our proteome analysis, that the amount of CS is down-regulated in *S. saprophyticus* after incubation in acid pH (with high availability of soluble iron), we investigated if CS activity is also

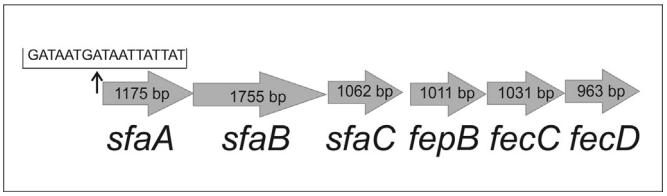

Fig. 3. Genetic map of the operon related to siderophore production in *S. saprophyticus*. The operon is composed by the biosynthetic machinery for the siderophore staphyloferrin A and its transporter. Open reading frames are indicated by arrows that show the direction of transcription. Size is indicated within the arrows (in base pairs). One putative region for ferric uptake regulator (Fur) ligation was identified and is shown (GATAATGATAATTATTAT). *sfaA*: ORF encoding MFS transporter, related to siderophore export; *sfaB*: ORF encoding siderophore synthetase containing luca/lucc motifs; *sfaC*: ORF encoding alanine racemase; *fepB*: ORF encoding the periplasmic component of ABC-type cobalamin Fe3+-siderophores transport system; *fepC*: ORF encoding inner component of iron-dicitrate ABC transporter permease; *fepD*: ORF encoding inner component of iron-dicitrate ABC transporter permease.

down-regulated in *S. saprophyticus* after incubation in acid pH. An enzymatic assay was performed and the result corroborates the proteomic analysis (Fig. 4, panel A). CS activity in *S. saprophyticus* protein extract after incubation in acid pH was around 0.15 μM of CoA formed per minute, and the CS activity measured in protein extract after incubation in alkaline pH was 33% higher (0.2 μM of CoA formed per minute). In order to detect if CS activity is increased in *S. saprophyticus* after incubation under conditions of iron deprivation, we also performed an enzymatic assay. Protein extracts were obtained after incubation of *S. saprophyticus* cells in SSD medium with and without iron, as described above. The results are shown in Fig. 4, panel B and show the iron deprivation increases in CS activity in 12 folds, suggesting that *S. saprophyticus* can use citrate for siderophore synthesis during iron limitation.

2.8. S. saprophyticus *produces siderophore after cultivation in iron-depriving conditions*

In order to verify if *S. saprophyticus* is really capable of producing siderophores, we performed siderophore detection after *S. saprophyticus* cultivation under iron-limiting conditions. The cells were cultured in SSD medium without iron and the culture supernatant was used to perform a CAS assay. The result is shown in Fig. 5, panel A. *S. saprophyticus* culture supernatant promoted a change in color, from blue to yellow, of CAS solution, suggesting that the bacteria produce carboxylate siderophores to obtain iron. In order to confirm the production of carboxylates by *S. saprophyticus*, a chemical assay was performed using phenolphthalein. The result is shown in Fig. 5, panel B. The change of color, from pink to yellow is caused by the change of pH promoted by carboxylates, confirming the presence of these siderophores in the *S. saprophyticus* culture supernatant.

3. Discussion

The adaptation of pathogens at the transcriptional level to variations in pH has been reported in other models, such as *S. aureus* and *Streptococcus mutans* [37,38]. However, a proteomic approach has not been reported in the study of bacterial metabolic adaptations to pH shift. *S. saprophyticus'* adaptation to variations in pH is important, since the bacterial cells are subjected to acid pH in the bladder in the first step of infection (urine pH ranges from 5 to 6), and after installation of infection, the pH increases in response to urea consumption and ammonia formation. Our results show that the down-regulation of lactic acid production occurs during acid incubation of *S. saprophyticus* cells (Supplementary Table 1). This response is also observed at the transcriptional level in *S. aureus* in response to inorganic acid shock. It probably occurs to avoid a decrease in pH since lactic acid promotes acidification [37]. In addition, we observed the up-regulation of two urease subunits in *S. saprophyticus* during acid incubation and down-regulation of three urease subunits during alkaline incubation (Supplementary Tables 1 and 2), which was also detected, at the transcriptional level, in *S. aureus* [37]. It is probably influenced by alkalization that occurs when urease converts urea into ammonia. The enzyme is up-regulated during acid incubation in order to promote an increase in the extracellular pH. Conversely, its down-regulation in alkaline conditions avoids further increasing of pH.

The most evident *S. saprophyticus* response to acid and alkaline pH was related to iron metabolism, including iron acquisition, storage and utilization (Table 1). This is understandable since iron solubility is affected by pH, and high concentrations of soluble iron are reached at acidic pH. The down-regulation of transcripts encoding proteins related to iron acquisition is also reported in *S. mutans* and probably also occurs due to the higher availability of soluble iron in this condition and to avoid damaging Fenton chemistry from occurring. In view of the indispensable nature of iron and its involvement in several key metabolic processes, including amino acid synthesis, TCA cycle, DNA replication, cellular respiration and electron transport, microorganisms possess sophisticated machineries to import, export and stock this metal. Thus, the common mechanisms of iron assimilation include the reduction of ferric (Fe^{3+}) to ferrous (Fe^{2+}), and acquisition of Fe^{3+} by binding siderophores [39]. In this way, *S. saprophyticus* must avoid iron toxicity in lower pH and adapt to avoid iron deprivation in alkaline pH.

In this work we show that *S. saprophyticus* cells previously deprived of iron exhibited reduced survival during macrophage interaction, suggesting that the metal is important during host-pathogen interaction (Fig. 2).

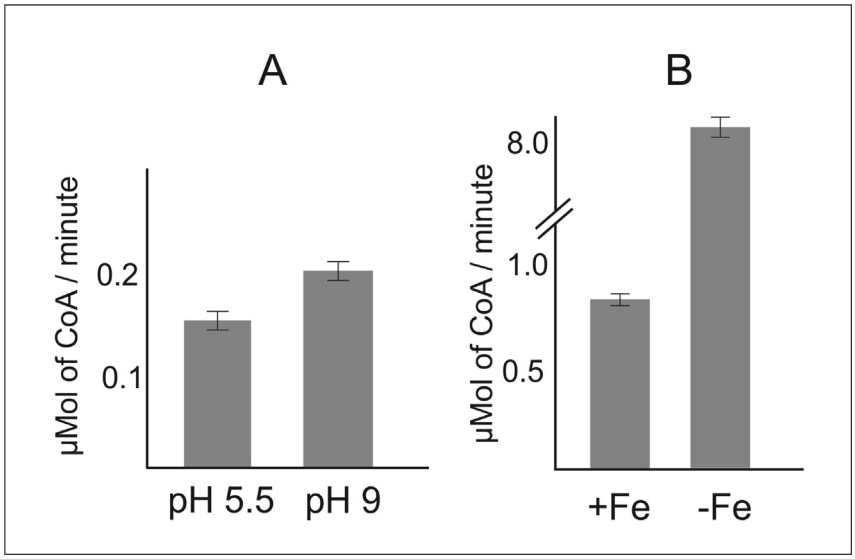

Fig. 4. CS enzymatic assay to evaluate citrate production at pHs 5.5 and 9 and during iron deprivation. (A) The CS enzymatic assay was performed using protein extracts from *S. saprophyticus* after incubation in the pHs used for proteomic analysis (5.5 and 9). (B) The enzymatic assay was also performed with *S. saprophyticus* protein extracts after incubation without iron (-Fe) and incubation with iron (+Fe) as used for comparison. The experiments were performed in triplicate and standard error of the mean obtained.

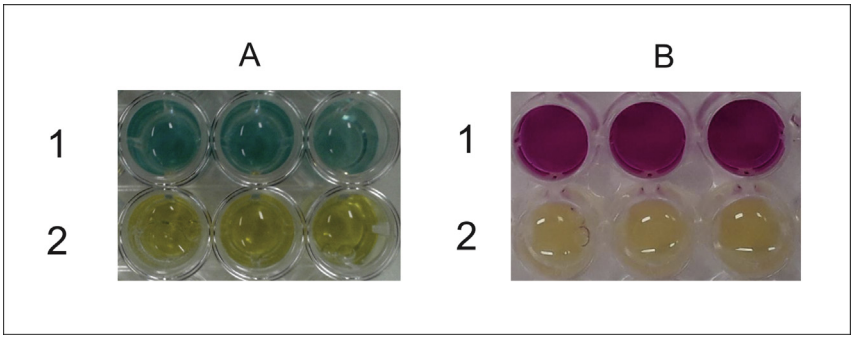

Fig. 5. Siderophore production of *S. saprophyticus* cells by using CAS assay. A: The CAS assay to detect siderophore production in the *S. saprophyticus* culture supernatant. The assay was performed after cell growth in SSD medium without iron to promote siderophore production. 1: Control CAS medium. 2: CAS assay using *S. saprophyticus* culture supernatant. The change of color (from blue to yellow) occurs in the presence of siderophores. The experiment was performed in triplicate, shown in Figure. B: Siderophore characterization by chemical assay using phenolphthalein. 1: Control phenolphthalein solution. 2: *S. saprophyticus* culture supernatant with phenolphthalein. The change of color (from pink to yellow) occurs in the presence of carboxylate siderophores.

Although the previous homology analyses (comparison of *S. aureus* operon for staphyloferrin B synthesis) state that *S. saprophyticus* does not possess the genomic machinery for siderophore synthesis [23], it was shown that *S. aureus* produces two siderophores (staphyloferrin A and B) by two distinct operons. These are metallophores that can bind to iron, zinc and other metals [17]. Until this moment, only operons for staphyloferrin A-like siderophores have been detected in coagulase negative *Staphylococcus* species, such as described in *S. epidermidis* [21]. In this context, we performed *in silico* analysis to detect if *S. saprophyticus* possesses machinery for staphyloferrin A-like siderophores. An operon was predicted, probably regulated by **F**erric **u**ptake **r**egulator (Fur), described as an iron transcriptional regulator (Fig. 3), suggesting that *S. saprophyticus* can produce siderophores by using this genomic machinery. Our *in silico* analysis was unable to detect an operon homologous to the *S. aureus* operon for staphyloferrin B synthesis, suggesting that *S. saprophyticus* possesses only one pathway to synthesize siderophores. It is important to highlight that, in *S. aureus*, the citrate used for staphyloferrin B synthesis is not produced by TCA CS. This organism possesses a second CS (SbnG) that is synthesized by the *sbnG* gene. Since we did not detect any gene that was homologous with *S. aureus' sbnG* (data not shown), we can suggest that *S. saprophyticus* uses CS from TCA to generate citrate for siderophore production. Of special note is the fact that the CS from TCA was detected in our proteomic analysis and was down-regulated after incubation of *S. saprophyticus* at acid pH, a condition that favors soluble iron. In order to validate this finding, we measured CS activity and we detected that *S. saprophyticus* presents lower CS activity at acid pH, compared to alkaline pH, corroborating our proteomic analysis (Fig. 4, panel A).

The production of siderophores by *S. aureus* is well known. Also, *S. aureus* possesses extracellular surface lipoproteins FhuD1 and FhuD2 and ABC transporter complex FhuCBG to facilitate the use of hydroxamate xenosiderophores [19]. Staphyloferrin A is transported by SfaA transporter, and SfaA mutant exhibited growth defects of 2.2-fold in A549 epithelial cells, suggesting that the efflux of metallophores is important during infection [40]. *S. epidermidis* requires iron to form biofilm, and cells deprived of iron are defective in the formation of biofilm [21].

We have evaluated, for the first time, whether *S. saprophyticus* is able to produce siderophores (Fig. 5, panel A). Our findings show that *S. saprophyticus* produces carboxylate siderophores (Fig. 5, panel B), and we suggest that these molecules are derived from citrate. In order to prove this suggestion, we evaluated the CS activity in *S. saprophyticus* after incubation in iron-depriving conditions. Our results show a high increase in CS activity during iron-limiting incubation (Fig. 4, panel B), showing that *S. saprophyticus* increases the availability of citrate during iron limitation, probably in order to increase siderophore production. This work is the first description of iron metabolism modulation during pH variation in *S. saprophyticus* and reports the synthesis of siderophores in this species. Our results suggest iron is important for bacterial survival during interaction with host cells, and consequently enhances the prospect for studies related to the importance of iron metabolism during infections caused by *S. saprophyticus*.

Conflict of interest

The authors declare no conflict of interest.

Acknowledgments

This work was supported by Conselho Nacional de Desenvolvimento Científico e Tecnológico (CNPq, process number 444662/2014-6) and Fundação de Amparo à Pesquisa do Estado de Goiás (FAPEG, Pronex). BSVS and KCSS was supported by a scholarship from Coordenação de Aperfeiçoamento de Pessoal de Nível Superior. This work is part of INCT of Strategies of Host-Pathogen Interactions (INCT-HPI)

Appendix A. Supplementary data

Supplementary data to this article can be found online at https://doi.org/10.1016/j.micinf.2019.04.008.

References

[1] Kloos WE, Bannerman TL. Update on clinical significance of coagulase-negative staphylococci. Clin Microbiol Rev 1994;7:117–40.
[2] Heikens E, Fleer A, Paauw A, Florijn A, Fluit AC. Comparison of genotypic and phenotypic methods for species-level identification of clinical isolates of coagulase-negative staphylococci. J Clin Microbiol 2005;43:2286–90.
[3] Raz R, Colodner R, Kunin CM. Who are you–*Staphylococcus saprophyticus*? Clin Infect Dis 2005;40:896–8.
[4] Weinberg ED. Nutritional immunity. Host's attempt to withhold iron from microbial invaders. Jama 1975;231:39–41.
[5] Bilitewski U, Blodgett JAV, Duhme-Klair AK, Dallavalle S, Laschat S, Routledge A, et al. Chemical and biological aspects of nutritional immunity-perspectives for new anti-infectives that target iron uptake systems. Angew Chem Int Ed Engl 2017;56:14360–82.
[6] Andreini C, Banci L, Bertini I, Rosato A. Occurrence of copper proteins through the three domains of life: a bioinformatic approach. J Proteome Res 2008;7:209–16.

[7] Corbin BD, Seeley EH, Raab A, Feldmann J, Miller MR, Torres VJ, et al. Metal chelation and inhibition of bacterial growth in tissue abscesses. Science 2008;319:962–5.
[8] Kehl-Fie TE, Chitayat S, Hood MI, Damo S, Restrepo N, Garcia C, et al. Nutrient metal sequestration by calprotectin inhibits bacterial superoxide defense, enhancing neutrophil killing of *Staphylococcus aureus*. Cell Host Microbe 2011;10:158–64.
[9] Gatermann S, John J, Marre R. *Staphylococcus saprophyticus* urease: characterization and contribution to uropathogenicity in unobstructed urinary tract infection of rats. Infect Immun 1989;57:110–6.
[10] Simandi L, Besenyei G. Kinetics and mechanisms of the reactions of transition metal complexes. Acta Pharm Hung 2000;70:244–50.
[11] Macara IG, Hoy TG, Harrison PM. The formation of ferritin from apoferritin. Inhibition and metal ion-binding studies. Biochem J 1973;135:785–9.
[12] Miethke M, Marahiel MA. Siderophore-based iron acquisition and pathogen control. Microbiol Mol Biol Rev 2007;71:413–51.
[13] Dimkpa CO, Svatos A, Dabrowska P, Schmidt A, Boland W, Kothe E. Involvement of siderophores in the reduction of metal-induced inhibition of auxin synthesis in *Streptomyces* spp. Chemosphere 2008;74:19–25.
[14] Diarra MS, Lavoie MC, Jacques M, Darwish I, Dolence EK, Dolence JA, et al. Species selectivity of new siderophore-drug conjugates that use specific iron uptake for entry into bacteria. Antimicrob Agents Chemother 1996;40:2610–7.
[15] Andrews SC, Robinson AK, Rodriguez-Quinones F. Bacterial iron homeostasis. FEMS Microbiol Rev 2003;27:215–37.
[16] Drechsel H, Freund S, Nicholson G, Haag H, Jung O, Zahner H, et al. Purification and chemical characterization of staphyloferrin B, a hydrophilic siderophore from staphylococci. Biometals 1993;6:185–92.
[17] Sheldon JR, Marolda CL, Heinrichs DE. TCA cycle activity in *Staphylococcus aureus* is essential for iron-regulated synthesis of staphyloferrin A, but not staphyloferrin B: the benefit of a second citrate synthase. Mol Microbiol 2014;92:824–39.
[18] Kobylarz MJ, Grigg JC, Sheldon JR, Heinrichs DE, Murphy ME. SbnG, a citrate synthase in *Staphylococcus aureus*: a new fold on an old enzyme. J Biol Chem 2014;289:33797–807.
[19] Endicott NP, Lee E, Wencewicz TA. Structural basis for xenosiderophore utilization by the human pathogen *Staphylococcus aureus*. ACS Infect Dis 2017;3:542–53.
[20] Massonet C, Pintens V, Merckx R, Anne J, Lammertyn E, Van Eldere J. Effect of iron on the expression of sirR and sitABC in biofilm-associated *Staphylococcus epidermidis*. BMC Microbiol 2006;6:103.
[21] Oliveira F, Franca A, Cerca N. *Staphylococcus epidermidis* is largely dependent on iron availability to form biofilms. Int J Med Microbiol 2017;307:552–63.
[22] Gokarn K, Pal RB. Activity of siderophores against drug-resistant Gram-positive and Gram-negative bacteria. Infect Drug Resist 2018;11:61–75.
[23] Kuroda M, Yamashita A, Hirakawa H, Kumano M, Morikawa K, Higashide M, et al. Whole genome sequence of *Staphylococcus saprophyticus* reveals the pathogenesis of uncomplicated urinary tract infection. Proc Natl Acad Sci U S A 2005;102:13272–7.
[24] Brock M, Buckel W. On the mechanism of action of the antifungal agent propionate. Eur J Biochem 2004;271:3227–41.
[25] Lindsay JA, Riley TV. Staphylococcal iron requirements, siderophore production, and iron-regulated protein expression. Infect Immun 1994;62:2309–14.
[26] Silva-Bailao MG, Bailao EFLC, Lechner BE, Gauthier GM, Lindner H, Bailao AM, et al. Hydroxamate production as a high affinity iron acquisition mechanism in *Paracoccidioides* spp. PLoS One 2014;9:e105805.
[27] Machuca A, Milagres AM. Use of CAS-agar plate modified to study the effect of different variables on the siderophore production by *Aspergillus*. Lett Appl Microbiol 2003;36:177–81.
[28] Dave BP, Dube HC. Chemical characterization of fungal siderophores. Indian J Exp Biol 2000;38:56–62.
[29] Alhasawi A, Castonguay Z, Appanna ND, Auger C, Appanna VD. Glycine metabolism and anti-oxidative defence mechanisms in *Pseudomonas fluorescens*. Microbiol Res 2015;171:26–31.
[30] Caza M, Kronstad JW. Shared and distinct mechanisms of iron acquisition by bacterial and fungal pathogens of humans. Front Cell Infect Microbiol 2013;3:80.
[31] Biswas L, Biswas R, Nerz C, Ohlsen K, Schlag M, Schafer T, et al. Role of the twin-arginine translocation pathway in *Staphylococcus*. J Bacteriol 2009;191:5921–9.
[32] Abdul-Tehrani H, Hudson AJ, Chang YS, Timms AR, Hawkins C, Williams JM, et al. Ferritin mutants of *Escherichia coli* are iron deficient and growth impaired, and Fur mutants are iron deficient. J Bacteriol 1999;181:1415–28.
[33] Kafala B, Sasarman A. Isolation of the *Staphylococcus aureus* hemCDBL gene cluster coding for early steps in heme biosynthesis. Gene 1997;199:231–9.
[34] Saini A, Mapolelo DT, Chahal HK, Johnson MK, Outten FW. SufD and SufC ATPase activity are required for iron acquisition during *in vivo* Fe-S cluster formation on SufB. Biochemistry 2010;49:9402–12.
[35] Nobre LS, Goncalves VL, Saraiva LM. Flavohemoglobin of *Staphylococcus aureus*. Methods Enzymol 2008;436:203–16.
[36] Wollers S, Layer G, Garcia-Serres R, Signor L, Clemancey M, Latour JM, et al. Iron-sulfur (Fe-S) cluster assembly: the SufBCD complex is a new type of Fe-S scaffold with a flavin redox cofactor. J Biol Chem 2010;285:23331–41.
[37] Anderson KL, Roux CM, Olson MW, Luong TT, Lee CY, Olson R, et al. Characterizing the effects of inorganic acid and alkaline shock on the *Staphylococcus aureus* transcriptome and messenger RNA turnover. FEMS Immunol Med Microbiol 2010;60:208–50.
[38] Baker JL, Abranches J, Faustoferri RC, Hubbard CJ, Lemos JA, Courtney MA, et al. Transcriptional profile of glucose-shocked and acid-adapted strains of *Streptococcus mutans*. Mol Oral Microbiol 2015;30:496–517.
[39] Sheldon JR, Heinrichs DE. Recent developments in understanding the iron acquisition strategies of gram positive pathogens. FEMS Microbiol Rev 2015;39:592–630.
[40] Nakaminami H, Chen C, Truong-Bolduc QC, Kim ES, Wang Y, Hooper DC. Efflux transporter of siderophore staphyloferrin A in *Staphylococcus aureus* contributes to bacterial fitness in abscesses and epithelial cells. Infect Immun 2017;85.